Research Article

Characterisation of Used PP-Based Car Bumpers and Their Recycling Properties

M. P. Luda,[1] V. Brunella,[1] and D. Guaratto[2]

[1] *Dipartimento di Chimica, NIS Centre of Excellence, Università di Torino, via Giuria 7, 10125 Torino, Italy*
[2] *Dipartimento di Chimica, Università di Torino, via Giuria 7, 10125 Torino, Italy*

Correspondence should be addressed to M. P. Luda; mariapaola.luda@unito.it

Three used PP-based car bumpers are characterized by many techniques (fractionation, IR, TGA, DSC, DMTA, and SEM). They show different impact and static and dynamic mechanical properties depending on their composition and morphology. It appears that block copolymer compatibilizers constituted by polyethylene-polypropylene sequences allow a better compatibility between the rubber domains and the PP matrix leading to relatively high impact resistance. Indeed if the ethylene sequences of the copolymer are large enough to crystallize, the decreased mobility of the whole system impairs the impact resistance. In addition, a higher amount of rubber in domains regular in shape and of greater dimension (1–3 μm) promotes a more homogeneous dispersion of external force inside the material, decreasing the risk of fracture. The amount of mineral fillers regulates the elastic modulus (the higher the load, the higher the modulus); however, a fairly good interfacial adhesion is required for satisfactory impact strength. All PP-based bumpers have been mechanically recycled in an internal mixer to redistribute oxidized species and to reestablish phase compatibilization. Recycling improves mechanical properties in slow speed test but fails to increase impact strength particularly in filled bumper, in which the quality of the matrix/filler interphase is hard to improve by simple remixing.

1. Introduction

Thermoplastic olefin elastomers (TPO) constitute the largest single market of the automotive field: excellent weatherability, low density, and relatively low cost make TPO as current material of choice for automotive bumpers and fascias. At the beginning of the years 2000, the automotive segments were using 7 million ton/yr of polymers and polypropylene based materials accounted for 41% [1]. In Italian cars in the years 2000, polymers contribute on average to 12% of the total weight and bumper contributes to 7%–10% of the plastic fraction [2].

TPO are blends of isotactic polypropylene (PP) with ethylene-propylene rubber (ethylene-propylene monomer, EPM, or ethylene propylene-diene monomer, EPDM). The production by in situ synthesis of specialty ethylene-propylene copolymers extended their uses in a wide range of applications: in the first section of the process PP or PP-rich copolymers are usually produced with a high molecular weight and medium crystallinity, and in the following

sections, copolymers richer in ethylene, an amorphous elastomeric material, are formed [3].

Front bumpers are made from neat TPO to take advantage from its elasticity whereas rear ones are often made from talc filled TPO to decrease production costs [4].

TPO are multiphase materials displaying a nodular morphology, where the EPM phase is dispersed in the form of spherical particles in PP matrix. Compatibilizers improve mechanical properties. Fillers can be dispersed in the PP matrix or embedded in the rubber particles depending on their size and surface treatment [5]. Performances of TPO systems strongly depend on their multiphase morphology which allows stress transfer among the PP/EPM interphase. In addition, clusters of badly dispersed mineral charges possibly act as crack propagators.

Due to high quotas of recover and reusing imposed by the ELV directive (95% of total weight by 2015, with 10%. max of energy recovery; End of Life Vehicles Directive 2000/53/EU) bumper reuse in a second market or an economical remunerative recycle strongly contributes to

comply with the recycling objectives to which the automobile manufacturers must subscribe. In order to better protect the environment, Directive 2008/98/EC takes measures for the treatment of ELV according to a hierarchy considering first prevention then preparation for reuse and recycling and eventually other recovery (notably energy recovery).

Aging of bumpers which occurred during their useful life causes oxidation of components and loss of compatibility at the interphase and progressive deterioration of damping properties. In principle mechanical recycling should be beneficial in terms of regaining original properties, reestablishing the phase compatibilization, and spreading the oxidized components in the whole mass [6, 7]; however, in practice, the final properties of recycled items often do not meet car bumpers requirements because of a not perfect reproduction of the original sophisticated morphology, which is a key point for superior performance.

Optical and mechanical properties of rubber-modified thermoplastics depend on the type and size of the rubber domains and on the glass transition temperature of the thermoplastic.

Many investigations have been carried out to elucidate the structure of the rubber phase [8–11], the morphology [11–15], and the role of the matrix [16] on the blend properties.

For instance, EPM synthesized using supported Titanium catalyst was mixtures ranging from random to progressively more blocky copolymers [8–10]: EPM synthesized by titanium-based traditional Ziegler Natta catalyst exhibited longer PE sequences that those synthesized by Vanadium-based catalyst [11].

The size of the rubber domains, their distribution, and uniformity are mostly governed by the preparation processes [17]. Viscosity of the blend components and shear rate in mixing affect the resultant morphology and the final properties: in general, a good dispersion of small rubber domains improves impact behavior [12, 14]; however larger rubber domains have been found to perform better in case of melt mixed blend [11]. Eventually, the rubber-matrix compatibilization is of relevance in determining the blend properties [12].

A successful recycling strongly depends on the process and on the use of appropriate additives and compatibilizers: regradative agents which link oxidized portions of polymer molecules to regain original molecular weight have been found nearly useless in such heterogeneous systems [18].

To regain original properties often mixing of used bumpers with variable amount of virgin polymer is performed [19]. Recently PP/EPM/nano $CaCO_3$ formulation appears in the market in the perspective of a simplified recycling [5] and minimizing the need of virgin polymer addition. However, automotive wastes stream still contains a huge amount of old TPO bumpers

In this work, three PP-based used bumpers of different composition, compatibilizer, and filler are mechanically and morphologically characterized to ascertain the effect of aging and the possibility to improve again their properties through reprocessing.
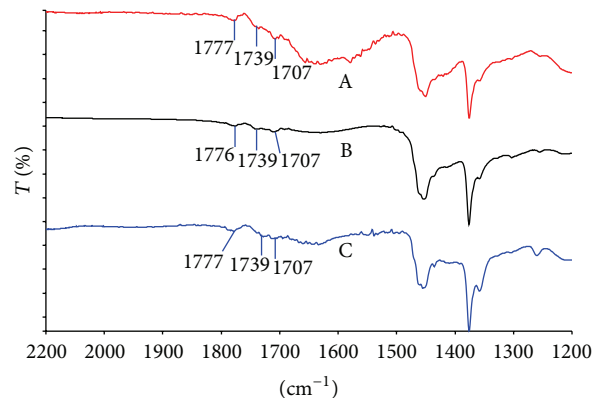

Figure 1: External surface oxidation (ATR) of used bumpers.

2. Materials and Methods

PP-based used bumpers were kindly supplied by ECO.DEM, a qualified car dismantler of Turin area, belonging to three different type of cars (sample A, sample B, and sample C). Their IR spectrum reveals similar amount of residual antioxidant (toluene extractable compound, showing $1739 \, cm^{-1}$ absorption) and negligible oxidation (no peaks at $1720 \, cm^{-1}$). An oxidative pattern (1776, $1707 \, cm^{-1}$ lactones and acids resp.) similar in all samples has been found only on the exposed surface of bumpers (Figure 1). Recycling was performed to redistribute oxidized species in the whole sample avoiding mechanical failure due to localized oxidation [16] in an internal mixer (Brabender AEV 330) at 220°C, 60 rpm for 10 min, adding 0.2% of Irganox B215 stabilizing package made by 2 parts of Irgafos 168 (tris-[2,4-di-tert-butylphenyl]-phosphite) and 1 part of Irganox 1010 (pentaerythrol tetrakis-3-[3,5-di-tert–butyl-4-hydroxyphenyl] propionate). Slabs were obtained by pressing the mixture at 220°C, 100 atm for 6 min followed by natural cooling. They are named AR, BR, and CR, respectively.

2.1. Characterization Techniques. Chemical structure, mechanical and physical properties, and morphology of used and rejuvenated bumpers were investigated by using the following techniques.

(i) Melt flow Index (MFI) was measured according to ISO 1133 (190°C).

(ii) Infrared analyses (IR) were run on Perkin Elmer Fourier Transform FTIR 2000 in transmission or in attenuated total reflection (ATR) method. Thin films for transmission measurements were prepared by cast film from xylene.

(iii) Elongational tests were performed at 10 mm/min (1.67×10^{-4} m/s) with a tensile test machines DY 22 (Adamel Lhomargy) on hollow punch-dumbbell shaped specimen, cut from original bumpers previously flattened for 30″ at 220°C and 130 atm or from rejuvenated plates. The average of 5 tests was considered. Secant E modulus was calculated (ε 0.025).

(a)

(b)

(c)
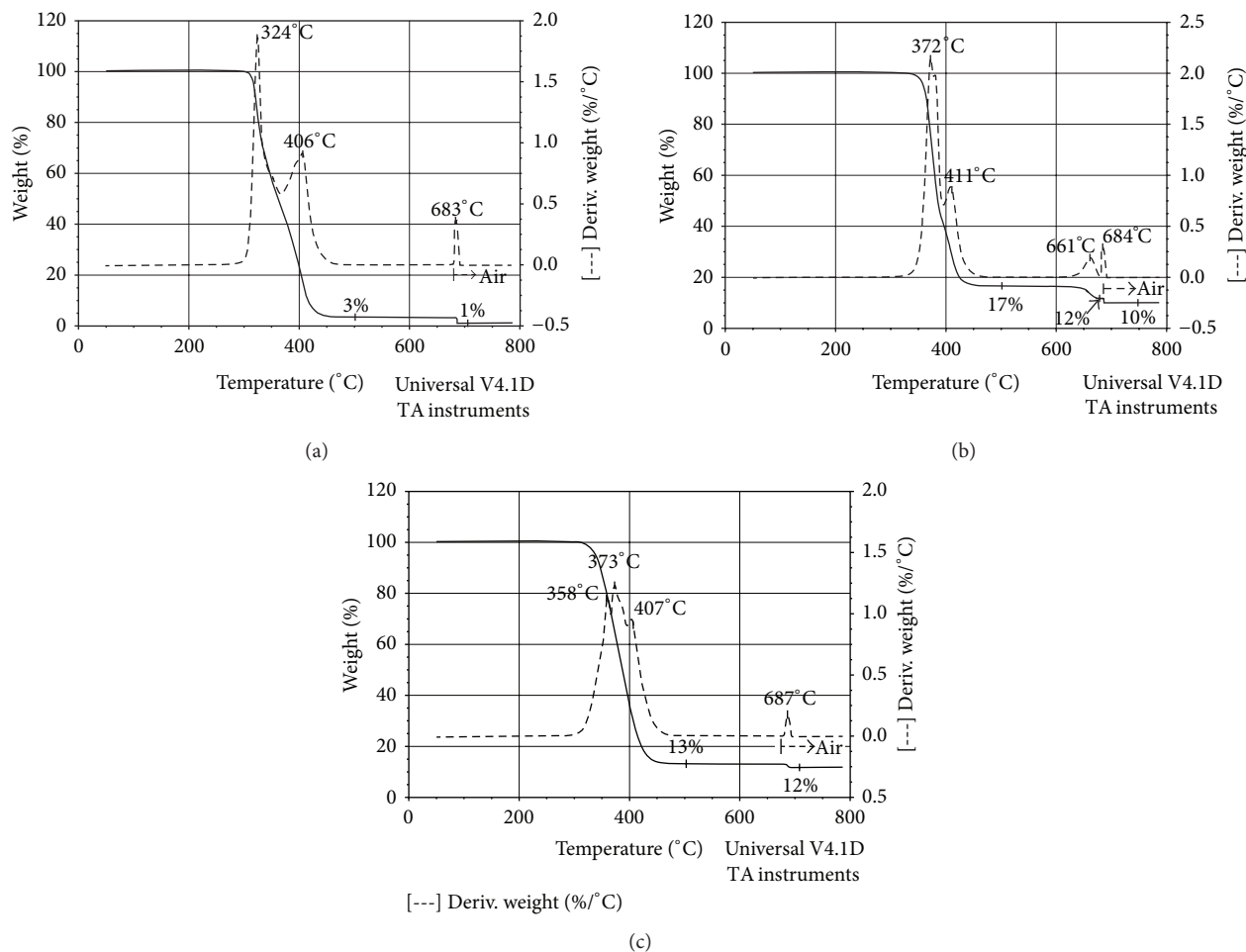
FIGURE 2: HRTGA of samples A (a), B (b), and C (c).

(iv) Charpy impact tests were carried out at room temperature according to ISO 179-2 using a CEAST Resil Impactor 25 J at estimated rate of 3.7 m/s. Samples size was 80 mm long, 10 mm thick, and 2.5 mm wide, and they were V 45° notched (with corner's ray of 2.5 mm) by a CEAST Motorized Notchvis. All measurements were carried out at room temperature.

(v) A Leica Stereoscan 420 SEM equipped with a secondary electron detector was used to examine surface of tensile and impact fracture. The samples were previously coated with gold by a sputter coater (BAL-TEC SCD 050) for 60 s under vacuum at a current intensity of 60 mA after mounting the sample on aluminum stubs with double-sided conductive tape.

(vi) A High Resolution Thermogravimetric Analyzer (HRTGA) TA Instrument Hi-res TGA 2950 thermobalance was used at 20°C/min up to 900°C, with a resolution factor +5 switching the atmosphere to air at 680°C to quantify carbon black (CB) by quick oxidation. 10–15 mg was used.

(vii) The melting behavior of polymers and copolymers was investigated by differential scanning calorimetry

(DSC 2010, TA Instruments) on about 10 mg samples cut from original bumpers or rejuvenated slabs by heating (20°C/min from 50°C to 220°C) in inert atmosphere.

(viii) The dynamic mechanical properties were determined in a TA Instruments DMA Q 800 equipped with CGA apparatus with a dual cantilever clamp at 1, 10.5, and 20 Hz. Samples (35 mm long, 2.5 mm thick and 12.5 mm wide) were cooled down to −120°C and heated at 3°C/min up to 100°C under a 30 μm controlled sinusoidal deformation. Specimens were directly cut from the flat part of the bumper or from the rejuvenated plates. The estimated error in the loss (E'') and the storage (E') moduli was ±4%. Area under tanδ peak (ATD) has been measured from the two adjacent minima.

3. Results

3.1. Bumper Composition. HRTGA of samples is shown in Figure 2. From these analyses, the amount of organic phase can be estimated as the difference from the original weight and the weight of the residue at 500°C, carbon black (CB)

TABLE 1: Composition of the used and rejuvenated bumpers.

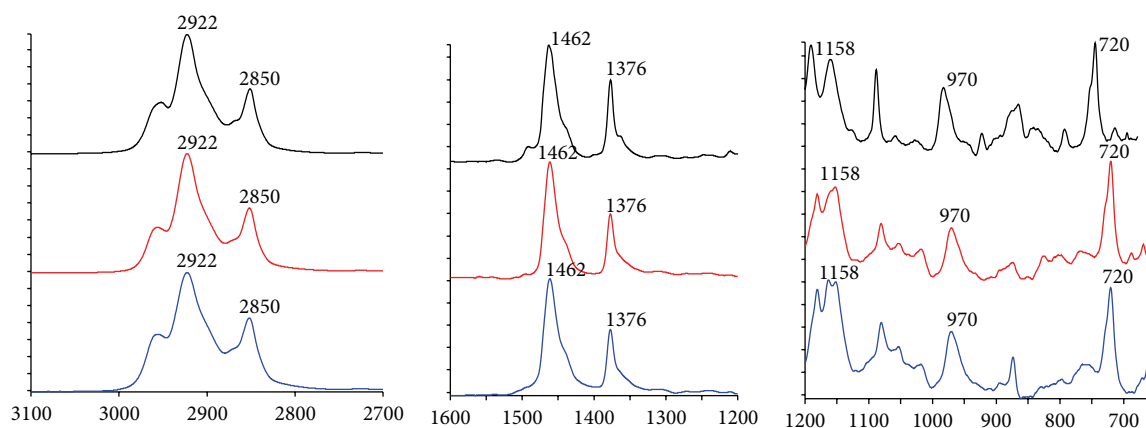|	Fraction soluble at 25°C [% w/w]	Fraction soluble at 75°C [% w/w]	Fraction soluble at 110°C [% w/w]	Cross-linked fraction [% w/w]	Inorganic fraction [% w/w]	Oxidable residue (carbon black [% w/w])
A,	17	19	61	tr	1	2
AR	19	22	56	tr	1	2
B	11	31	40	1	15	2
BR	9	32	41	1	15	2
C,	9	30	47	1	12	1
CR	9	30	46	2	12	1

tr: traces.

FIGURE 3: IR spectrum of the phase soluble at room temperature for samples A (top line), B (middle line), C (bottom line).

from the weight loss soon after the introduction of air in the system, and inorganic load from the final residue. According to that sample A contains 97% of organic phase, 2% of CB, and only traces of mineral load. Sample B contains 83% of organic phase, 2% of CB, and 15% of inorganics (11% of which is $CaCO_3$, resulting from the 5% weight loss at 661°C imputed to CO_2 evolution from $CaCO_3$). Sample C contains 87% of organic phase, 1% of CB, and 12% of mineral charge. Similar results were found on rejuvenated samples.

IR spectra of the residue at 550°C confirm the presence of $CaCO_3$ and talcum in B and of talcum in C, whereas A shows a negligible amount of residue.

The different shape of degradation of the organic phase in the three samples shown in Figure 2 reflects a difference in their composition. Therefore, separation of samples into fractions was performed to characterize the different phases which bumpers are made of. Three progressive phases have been isolated by their different solubility in xylene with the following procedure.

1 g of material was dissolved in xylene in a round bottom flask at 140°C and maintained at such a temperature for 30′ under stirring. Then, the bath was cooled down very slowly to 25°C and kept at this temperature for about one day. Precipitation and further sedimentation of a solid phase occurred which was isolated from the liquid phase and weighted. After evaporating the solvent, an IR spectrum was performed on the soluble phase. In the same way, a second

and a third extractions were performed on the residue of the previous extraction fixing the cooling temperatures at 75°C and 110°C, respectively. The cross-linked material and the charges remained in the residue.

To confirm the amount of crosslinked material, 0.5 g of each sample was put in a porous cellulose thimble dipped into xylene at 140°C for 48 h allowing soluble material to leach out of the thimble; the residue inside the thimble was weighted, and the amount of crosslinked material was calculated by subtracting the load of inorganic and oxidable charges of each sample resulting from HRTGA. TGAs were also performed on these residues to confirm the amount of organic (crosslinked material + CB) and inorganic filler determined above. As expected, similar results have been obtained by fractioning the rejuvenated bumpers; Table 1 summarizes the bumpers' composition.

3.2. Infrared Analyses. IR spectrum of the fraction soluble at 25°C is strictly similar for all the three samples (Figure 3). Absorptions at 1158 and 970 cm^{-1} are associated to ω and ρ vibrations of amorphous PP [20]. A single absorption at 720 cm^{-1} due to amorphous PE can be appreciated [6, 8, 20]. All that suggests that this fraction is amorphous EPM.

The IR spectra of Figure 4 are those of the fraction soluble at 75°C. Sample A exhibits an elevated amount of propylene units (absorption at 2950, 2867, and 1376 cm^{-1}, due to CH_3 stretching and bending) and strong absorptions at 1166, 997,
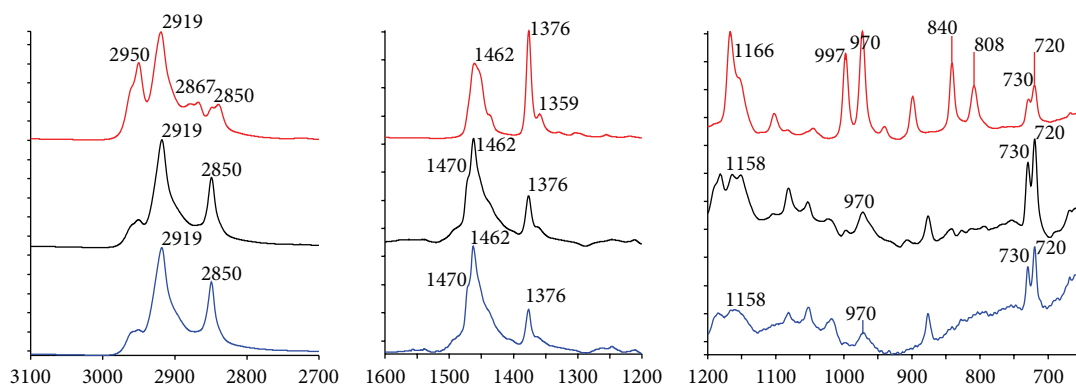
FIGURE 4: IR spectrum of the phase soluble at 75°C for samples A (top line), B (middle line) and C (bottom line).
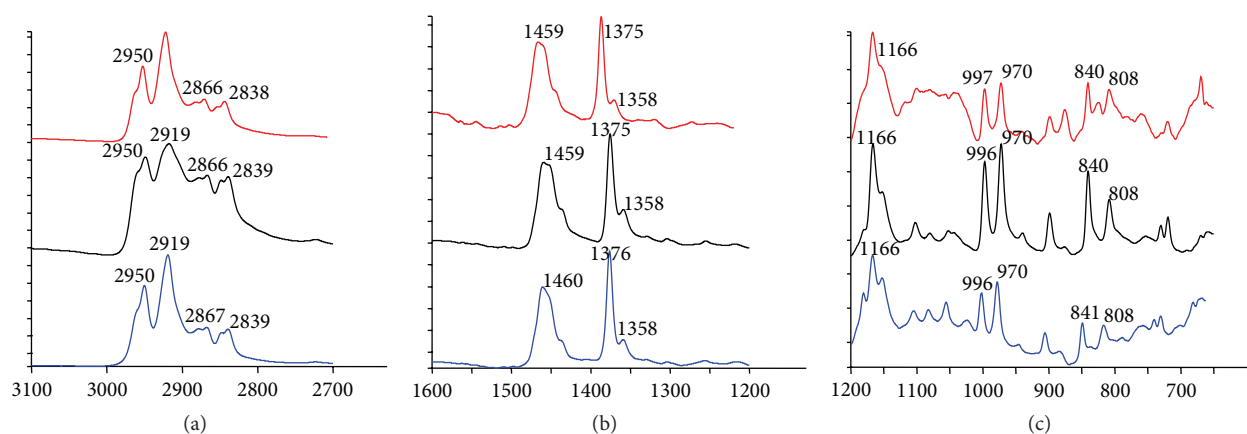

(a)　　　　　　　　　(b)　　　　　　　　　(c)

FIGURE 5: IR spectrum of the phase soluble at 110°C for samples for samples A (top line), B (middle line) and C (bottom line).

840, and 808 cm^{-1} which are negligible in the IR of B and C. Absorption at 808 cm^{-1} concerns CH$_2$ rocking in head-tail structure of PP; those at 1166, 997 and 840 cm^{-1} are attributed to the methyl rocking models associated with threefold helix of isotactic PP, which is the characteristic structure of PP crystals [20]. On the other hand, the absorptions due to amorphous PP (1158 and 970 cm^{-1}) are appreciable in all spectra, whilst a double peak at 720–730 cm^{-1} indicates the presence of crystalline PE [20]. PE crystallinity can be also appreciated from a shoulder at 1470 cm^{-1} [20] particularly evident in samples B and C. The broad shape of the 970 cm^{-1} band in B and C suggests that scattered units of propylene are distributed along mainly polymethylene units [20]. Therefore the fraction soluble at 75°C is an ethylene block copolymer with scattered units of propylene (PE/P) in samples B and C and a block (ethylene-propylene) copolymer (PP-PE) in sample A.

All peaks in the spectrum of the fraction soluble at 110°C are due to amorphous and crystalline isotactic PP, whereas peaks due to either amorphous or crystalline PEs are negligible; so, this fraction is PP (Figure 5).

For samples B/BR and C/CR the residual insoluble fraction is constituted by crosslinked PP CB, and inorganic fillers.

TABLE 2: MFI of original and rejuvenated bumpers (g/10 min).

	A	B	C
Original	5.7	5.9	6.6
Recycled	4.7	5.6	7.1

3.3. MFI. MFI is reported in Table 2. A and B show a similar melt viscosity despite the high amount of filler in B; C exhibits the highest MFI notwithstanding its high filler loading. Recycling caused a further decrease of viscosity in C and an increase in A and B.

3.4. DSC. Melting temperatures and value of peak integration from DSC of used and recycling bumpers are reported in Table 3, where the reported values of $\Delta H^{\text{melting}}$ are corrected for the presence of the inorganic fillers in B and C. The amount of PE crystallinity is much larger in B ($\Delta H^{\text{melting}}$ 5 J/g) than in C (1 J/g) and negligible in A. Further, the average size of the PE crystallites is larger in B than in C (Tm 125 and 115°C, resp.) indicates longer PE segments in the sequential copolymer of B (fraction soluble at 75°C).

TABLE 3: Melting temperatures and ΔH of PE and PP crystallites in bumpers determined by DSC.

	Melting PE $\Delta H^{\text{melting}}$ [J/g][a]	Melting PE $T_{\max}$ [°C][a]	Melting PP $\Delta H^{\text{melting}}$ [J/g][a]	Melting PP $T_{\max}$ [°C][a]
A	<1	nd[b]	43	170
AR	<1	nd[b]	34	175
B	5	131	50	166
BR	4	132	45	170
C	1	124	48	168
CR	1	125	41	171

[a] $\Delta H^{\text{melting}}$ [J/g] refers only to the weight of the organic part of the bumper.
[b] nd: not detectable.

TABLE 4: Tensile properties (20°C).

	Young modulus [MPa]	Elongation at break [%]
A	236 ± 16	85 ± 4
AR	226 ± 10	176 ± 10
B	274 ± 6	55 ± 4
BR	237 ± 20	107 ± 45
C	260 ± 17	20 ± 3
CR	242 ± 30	14 ± 2

The PP whole crystallinity in original bumpers is similar in B and C ($\Delta H^{\text{melting}}$ 50 and 48 J/g) and larger than that in A (43 J/g), possibly cause the nucleating power of the filler.

DSC of AR, BR, and CR shows features similar to those of used bumper; however because of the different processing conditions, $\Delta H^{\text{melting}}$ of PP is here smaller (lower crystallinity) and the melting temperatures are larger (larger size crystallites). Slightly larger crystallites are formed in PE after remixing (Table 3).

3.5. Tensional Properties. Results of quasistatic tensile tests are reported in Table 4. As expected, secant modulus depends on the amount of inorganic charge (IC) and increases with increasing loading (A: 236 MPa; B: 274 MPa; IC 15%; C: 260 MPa; IC12%); elongation at break shows relatively high values in A and B (ca. 85% and 55%, resp.) whereas C breaks under poor strain (ca. 20%). The deformation process is accompanied by stress whitening which becomes more intense as the test proceeds. Particularly in sample C, the cross-sectional areas of samples change very little between the yield points, and the failure indicating that crazing, rather than shear yielding, is most probably the dominant mode of deformation.

Recycling lowers % crystallinity and reduces modulus (AR: 226 MPa; BR: 237 MPa; CR: 242 MPa) but doubles elongation at break in AR and BR (176% and 107%, resp.) which however remains poor for sample C (14%). SEM micrographs of tensile fracture surface (Figure 6) are in agreement with such finding; samples A and B exhibit drawn material indicating an extensive plastic deformation occurring during the fracture, whereas in sample C the evident surfaces of fracture point to a fragile behavior with evidence of debonded particles of mineral charge.

3.6. DMTA. Dynamic Mechanical Thermal Analysis (DMTA) allows determination of the storage modulus E', the loss modulus E'', and the dissipation factor tanδ ($=E''/E'$). E' is related to the recoverable elastic energy stored in the sample; E'' is related to the deformation energy dissipated as heat of friction (by shearing or crazing mechanisms); the value of tanδ is a measure of the fraction of energy lost per cycle and is considered indicative of the damping properties of the material: the larger E'' (pronounced dissipation) and/or the smaller E' the higher the values of tanδ.

On the basis of tanδ peak (at 10.5 Hz), four transitions can be envisaged (Figure 7) attributed to the following relaxation phenomena [19–21]:

(i) at T comprising from -150°C to -100°C, a broad relaxation peak attributed to local rotary motion of ethylene sequences (δ relaxation);

(ii) at $T = -36/-38$°C, EPM copolymer's glass-rubber transition (γ relaxation);

(iii) at $T = 13$°C/16°C, amorphous PP's glass-rubber transition (β relaxation);

(iv) at $T > 100$°C, a shoulder attributed to a lamellar slip mechanism and rotation in the crystalline PP phase (α relaxation).

Each transition temperature raises when measured at higher frequencies, as expected; however, each transition (at the same frequency) occurs nearly at the same temperature for all samples (Figure 7). In Figure 8, tanδ and E'' values for γ and β transitions at 10.5 Hz are synoptically reported showing marked differences among the samples, whereas recycling of each sample only causes minor differences.

In γ transition, B/BR exhibit a value of tanδ (0.038-0.039) which is nearly half of those of the two others (0.063–0.068) (Figure 8(a)) despite that E'' is only slightly lower (Figure 8(b)) indicating that E' (B/BR) is much higher at this temperature and that the rubber phase of this sample displays a more elastic behavior. On the contrary, the rubber phase in C/CR shows the highest values of E'' (204–179 MPa) and the higher dissipating ability.

In β transition, all samples show comparable damping properties (tanδ, Figure 8(a)) despite the lower E'' in A/AR and C/CR (poorer dissipation capacity, Figure 8(b)) revealing an even smaller E' value.

δ transition is scarcely visible in A/AR and C/CR and negligible in B/BR. (Figure 7) This could be ascribed to the higher tendency to crystallize longer PE segments in B/BR as shown by DSC.

3.7. Impact Strength and Morphology. For PP-based bumpers a resilience above 35 KJ/m^2 is desirable [19]. Results of Charpy notched impact strength (NIS) test are reported in Table 5. The used samples do not meet such a requirement; however, there are remarkable differences amongst them which should
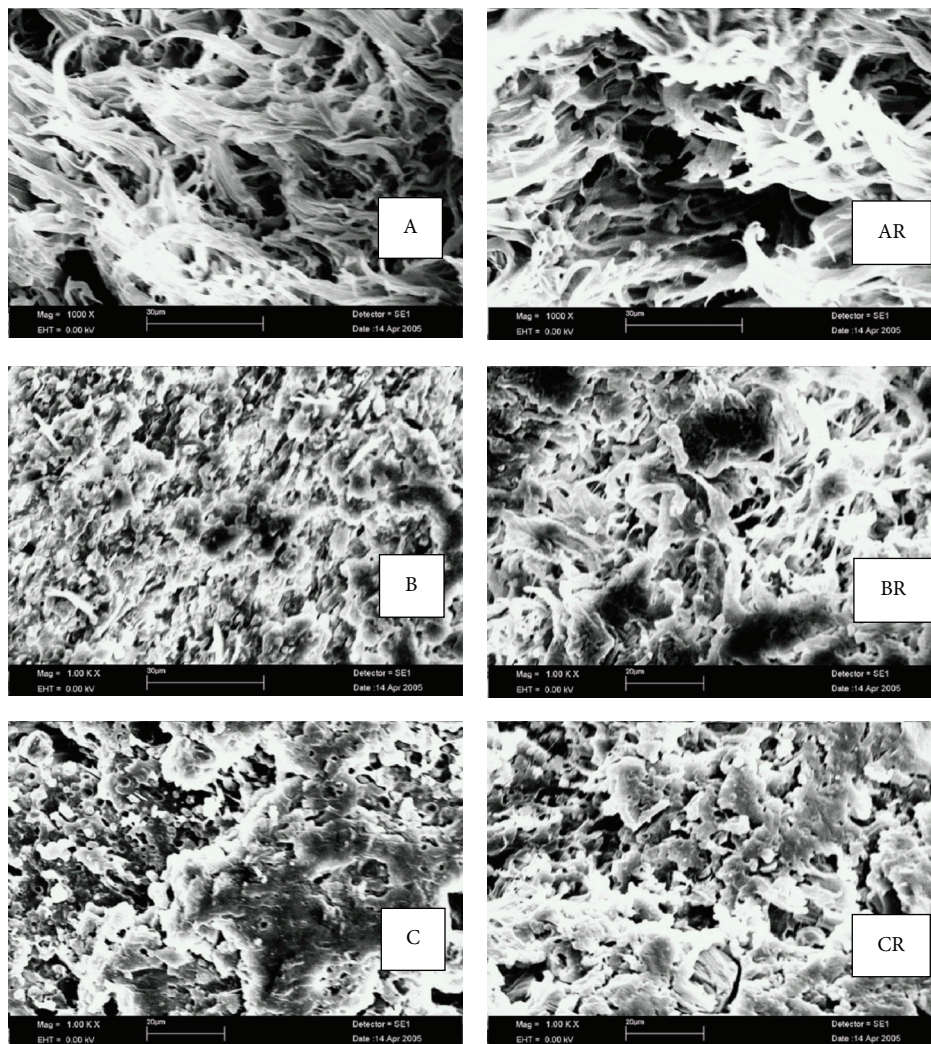
FIGURE 6: SEM micrographs of tensile fractured surface of samples A, AR, B, BR, C, and CR.

TABLE 5: Charpy test values.

	Resilience [KJ/m^2]	Peak strength [N]	Peak deformation [mm]
A	24.0 ± 4.0	107 ± 4	5.7 ± 0.3
AR	25.1 ± 0.4	95 ± 5	5.9 ± 0.7
B	5.0 ± 0.7	101 ± 5	2.2 ± 0.1
BR	6.0 ± 1.7	99 ± 5	2.1 ± 0.4
C	9.3 ± 1.3	93 ± 3	3.5 ± 0.1
CR	5.7 ± 0.9	76 ± 3	2.6 ± 0.5

be connected to their structure and morphology: A displays the highest resilience and highest deformations, B the lowest ones, the impact behavior of C being only slightly better than that of B. Recycling does not improve impact behavior, as already noticed [16], and tends to decrease further the impact resistance of C indeed.

It has been reported that in rubber modified PP systems tanδ values are linearly related to impact strength [21]; however, this does not hold presently, where B and C also contain inorganic charges; more recently good correlation was figured out between the area under tanδ (ATD) peaks and NIS [22, 23]. ATD represents the additional damping ability developed in the material due to the thermal transition; these values are synoptically reported in Figure 9 for γ and β relaxations. In impact condition at room temperature energy absorption should be mainly supported by EPM chains whose Tg is located at about −40°C. This is the case for A/AR (high γATD and high NIS) and B/BR (low γATD and low NIS); however, C/CR which exhibits a relatively high γATD has a scarce resilience indeed. On the other hand, the high βATD of B/BR does not improve NIS because the contribution of PP motion (Tg 13–16°C) to impact energy absorption at room temperature should be scarce.

Therefore, neither γATD nor βATD alone can explain the impact behavior of such complex systems because interrelation between the different phases, scarcely revealed by DMTA, plays a fundamental role in impact properties.

3.8. SEM. Micrographs of Charpy fractured impacted zones reported in Figure 10 show that in all samples the rubber
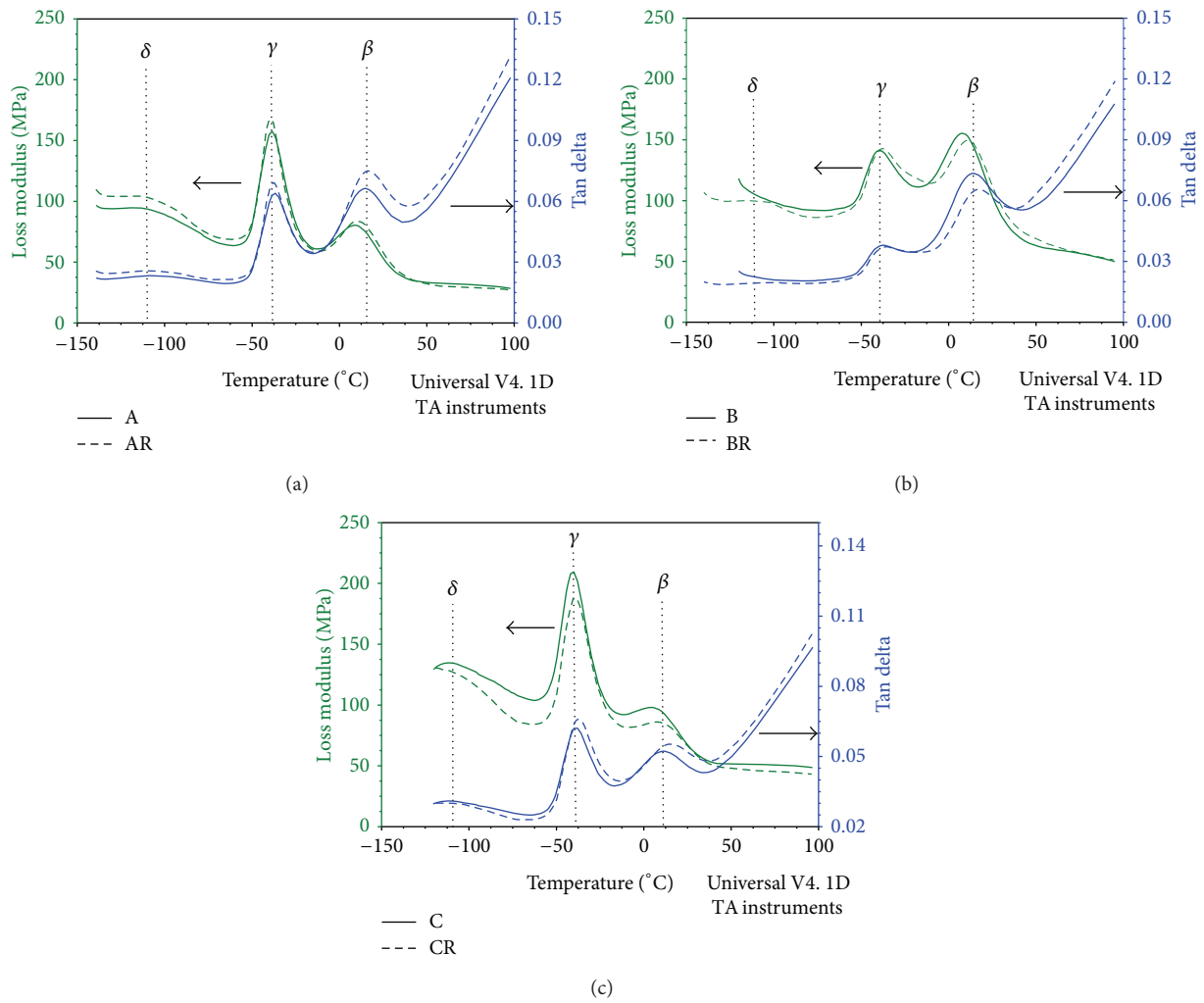
(a)

(b)

(c)

FIGURE 7: $\tan\delta$ and E'' measured at 10.5 Hz in DMTA of A/AR, B/BR, and C/CR.
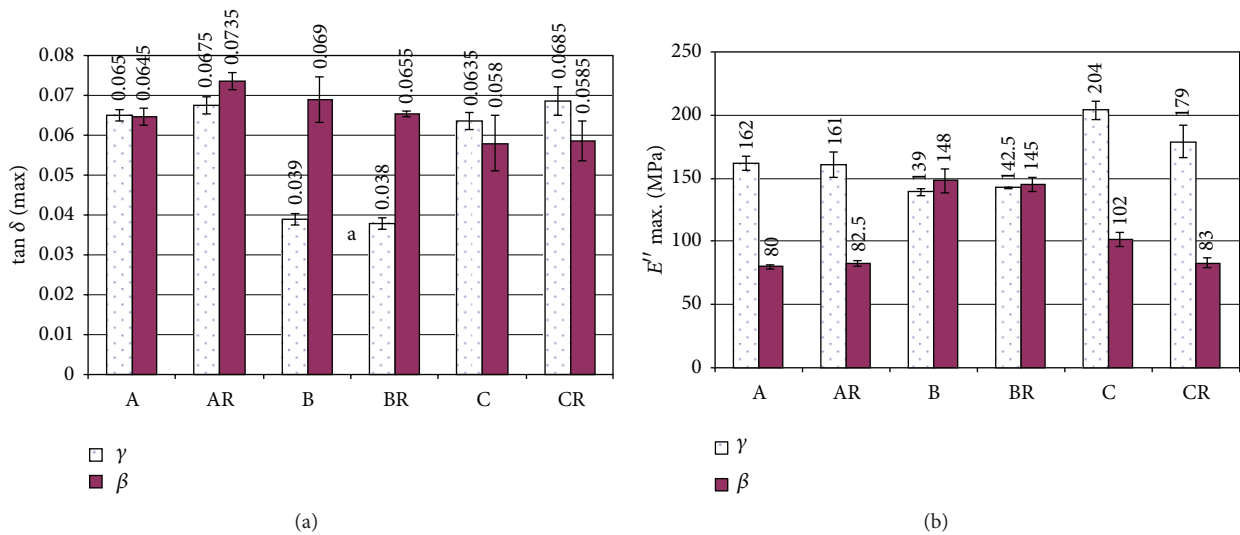

(a)

(b)

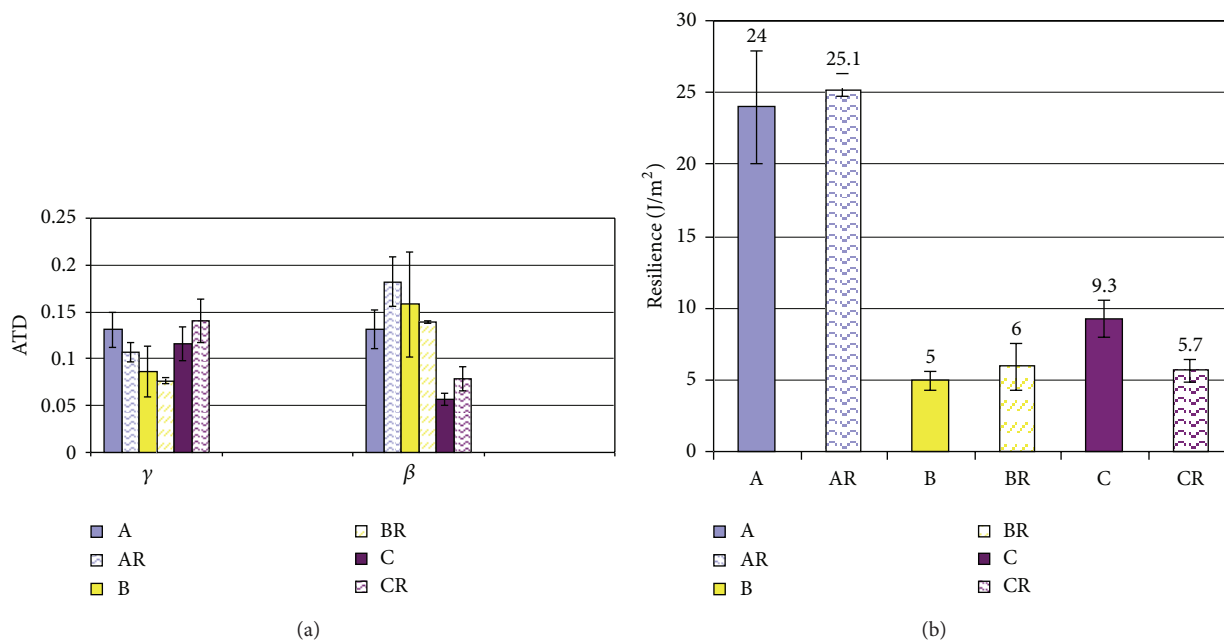FIGURE 8: DMTA of samples A/AR, B/BR, and C/CR measured at 10.5 Hz: maximum of $\tan\delta$ (a) and E'' (b).

FIGURE 9: (a) Area under tanδ from DMTA of A/AR, B/BR, and C/CR measured at 10.5 Hz; (b) Charpy resilience at room temperature for the same samples.

phase is constituted by round EPM domains dipped into the PP matrix. The size is bigger (range 2-3 μm) and more regularly distributed in A than in B (0.8–1.3 μm) and C (0.5–1.0 μm), in agreement with D'Orazio and coworkers [11] who found that long sequences of ethylene units in the copolymer led to smaller rubber domains. Recycling does not modify significantly the observed morphology which is mainly governed by phase viscosity and type of compatibilizer. The continuous PP phase appears globally intact in A and B whereas shows evident fracture in C. After impact, there are still some rubber domains jointed with the matrix in A while those of B and C have been cut and pulled away from the matrix. Hence, the matrix/rubber compatibility is far better in sample A than in the two others and induces effective energy absorption by self-cavitation of the rubbery domains. This different behavior could be associated with the different copolymers which bumpers are made with: block PE-PP copolymer (sample A) improves the compatibility EPM/PP better than copolymer made by PE sequences with PP scattered units (samples B, C) because PP segments in the segmented copolymer are highly compatible with the matrix and can induce formation of very small domains of a finely dispersed PE phase in PP, with improvement in impact strength [10, 12]. In addition, the largest deformation occurring under stress at the equator of the rubber particles acts as a stress concentrator relieved by crazing, a mechanism of energy absorption which is less efficient if particles are too small [17].

Micrographs also show debonding of inorganic charges occurring in B/BR, which are completely drawn out of the matrix in C/CR. As a general rule in notched impact tests the more the filler present the greater the number of obstacles a crack has to circumvent and the higher the impact

strength [17]. Hard fillers block the flow of the matrix under deformation both introducing constraints on the segmental mobility of the polymeric molecules and slowing the lamellar movement down at relaxation temperature, leading to a stiffer, stronger, tougher material [24, 25]. This has not been experienced in the present case: while a too strong adhesion between filler and matrix allows the cracks to propagate easily in the matrix resulting in a poor impact strength [17], on the other hand, a too weak interfacial adhesion between filler and PP as observed in B/BR and C/CR does not promote stress transfer from the matrix during loading resulting again in very poor NIS [25]. Impairment of the charge/PP interfacial adhesion could be an effect of ageing which appears not to be recovered by simple remixing.

4. Conclusions

While different used bumpers show reduced impact resistance there are many differences in their mechanical behavior which can be related to their composition and morphology. Full range investigations of composition and morphology, all together, have pointed out some aspects in structure-properties relationship in PP-based bumpers.

The role of the segmented/block copolymer mainly acting as a phase compatibilizer is of paramount relevance to the impact performance of bumpers. It appears that a block copolymer constituted by long PE-PP sequences (sample A) allows a better compatibility between the rubber domains and the PP matrix (Figure 10) leading to relatively high impact resistance. In addition a higher amount of rubber in domains regular in shape and of greater dimension (1–3 μm) promotes a more homogeneous dispersion of external force inside
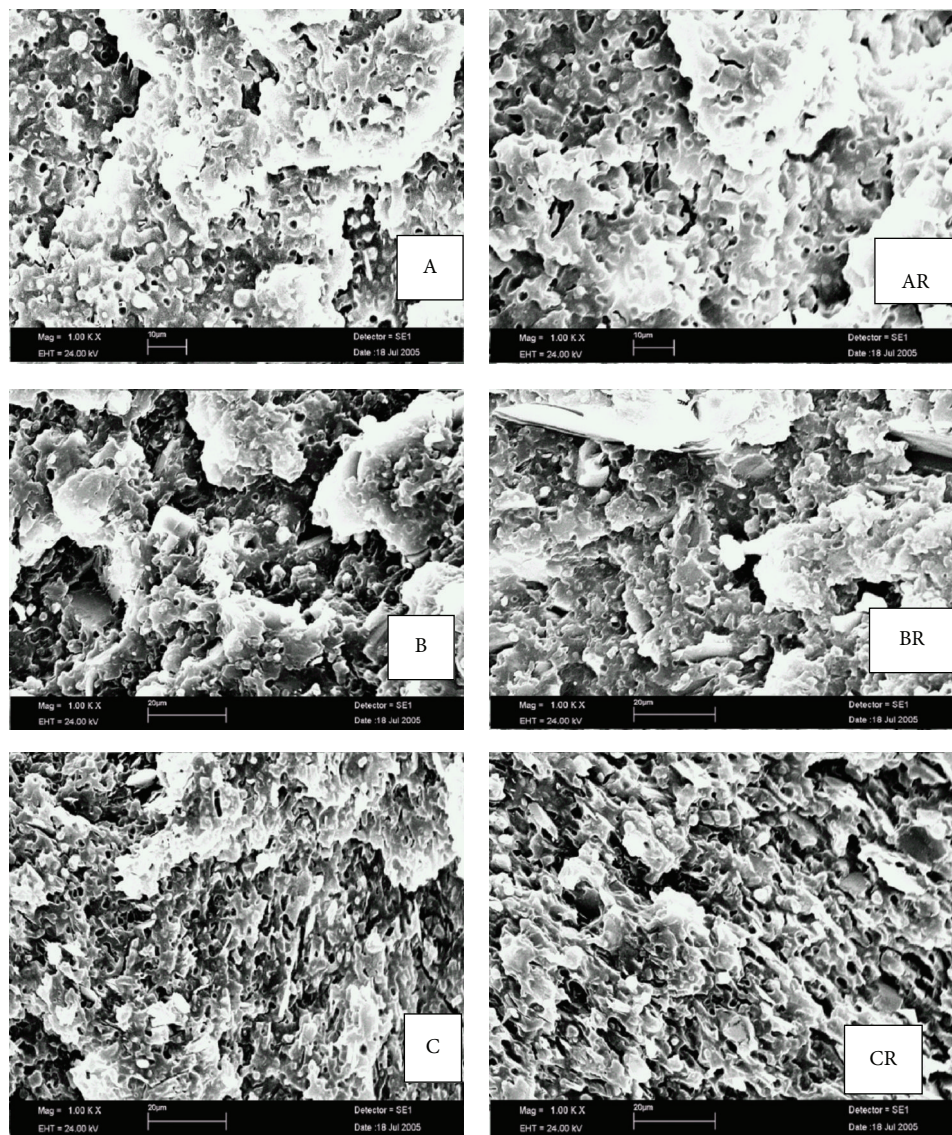
FIGURE 10: SEM micrographs of Charpy fractured surface of sample A, AR, B, BR, C, and CR.

the material, decreasing the risk of generating super-stressed points where fracture can easily set up and propagate.

In low speed test, in the cases of A and B, the thermoplastic matrix contributes to energy dissipation through yielding and shear deformation (Figure 7); on the contrary, a crazing mechanism is exhibited in C, due to a poorer matrix/rubber compatibility.

By contrast, the above mechanism of energy dissipation is not efficient in high speed test. Indeed in B, the ethylene sequences of the copolymer are large enough to crystallize, decreasing the mobility of the whole system impairing even more the impact resistance.

The amount of mineral fillers regulates the elastic modulus (the higher the load, the higher the modulus B > C > A); however, a fairly good interfacial adhesion is required for satisfactory impact strength.

Recycling by remixing in an internal mixer does not affect morphology (mainly dictated by viscosity of the components and kind of compatibilizer), redistributing compatibilizer (in principle reestablishing phase compatibilization) and the localized oxidations (which can act as fracture initiators).

In effect recycling strongly increases tensile properties in quasistatic tests doubling elongation at breaks in A and B but has no effect on C, the sample with the higher MFI and the worse interphase PP/EPM.

Nevertheless recycling fails to further increase impact properties even in those samples which exhibited an improved tensile behavior in low speed test (samples A and B).

As shown in Figures 6 and 10, remixing is not able to redistribute mineral charges in samples B and C because the charge/PP interfacial adhesion damaged by ageing is

not recovered by simple remixing. In effect the strength of the filler/matrix adhesion is usually obtained by chemical reactions [25] and is a critic parameter for impact properties.

Concerning the lack of impact properties improvement of unfilled sample A, an explanation could be that a limited thermooxidation of the matrix and/or the rubber can occur in recycling (even in the presence of antioxidants) leading to an inadequate rubber/matrix interface, suggesting to select very mild remixing condition.

Used bumpers constitute a well-defined waste stream collected separately from other wastes; however, bumpers have different composition, in particular they can be filled with mineral charge or unfilled and can present different composition of the polymeric fraction (matrix, rubber, and compatibilizer) and different level of ageing.

As a final consideration while a bumper-to-bumper recycling would be the better choice to comply with ELV regulation, this objective is presently still hard to reach and to this aim recycle has to be performed by the addition of considerable amount of virgin matrix. Other ways bumper can be recycled to less-demanding properties items. Filled bumpers are even hard to successfully recycling and the new formulations containing well-compatibilized nanocharges [5] can be a good solution for recycling future bumper waste stream.
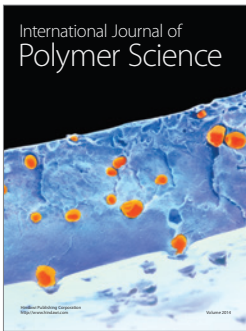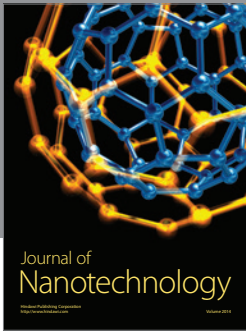
Acknowledgment

References

[1] P. Léna, "Le plastique, toujours plus fantastique," *Info Chimie Magazine*, vol. 42, no. 463, p. 44, 2005.

[2] "A.N.P.A. (Agenzia nazionale per la protezione dell'ambiente, O.N.R. (Osseevatorio Nazionale dei Rifiuti) I rifiuti del comparto automobilistico," Studio di settore, 2002.

[3] M. Pegoraro, F. Severini, L. Di Landro, R. Braglia, and J. Kolarik, "Structure and morphology of a novel ethylene-propylene copolymer and its blends with poly(propylene)," *Macromolecular Materials and Engineering*, vol. 280-281, pp. 14–19, 2000.

[4] M. Szostak, "Recycling of pp/epdm/talc car bumpers," *Chemicke Listy*, vol. 105, no. 15, pp. s307–s309, 2011.

[5] N. Mnif, V. Massardier, T. Kallel, and B. Elleuch, "New (PP/EPR)/nano-$CaCO_3$ based formulations in the perspective of polymer recycling. Effect of nanoparticles properties and compatibilizers," *Polymers for Advanced Technologies*, vol. 21, no. 12, pp. 896–903, 2010.

[6] R. Gallo, L. Brambilla, C. Castiglioni et al., "Environmental degradation of a novel ethylene-propylene copolymer in thick sheets," *European Polymer Journal*, vol. 41, no. 2, pp. 359–366, 2005.

[7] M. P. Luda, G. Ragosta, P. Musto et al., "Natural ageing of automotive polymer components: characterisation of new and used poly(propylene) based car bumpers," *Macromolecular Material Engeenering*, vol. 287, no. 6, pp. 404–411, 2002.

[8] C. Hongjun, L. Xiaolie, M. Dezhu, W. Jianmin, and T. Hongsheng, "Structure and properties of impact copolymer polypropylene. I. Chain structure," *Journal of Applied Polymer Science*, vol. 71, no. 1, pp. 93–101, 1999.

[9] Q. Dong, Z.-Q. Fan, Z.-S. Fu, and J.-T. Xu, "Fractionation and characterization of an ethylene-propylene copolymer produced with a $MgCl_2/SiO_2/TiCl_4$/diester-type ziegler-natta catalyst," *Journal of Applied Polymer Science*, vol. 107, no. 2, pp. 1301–1309, 2008.

[10] Z. Q. Fan, Y. Q. Zhang, J. T. Xu, H. T. Wang, and L. X. Feng, "Structure and properties of polypropylene/poly(ethylene-co-propylene) in-situ blends synthesized by spherical Ziegler-Natta catalyst," *Polymer*, vol. 42, no. 13, pp. 5559–5566, 2001.

[11] L. D'Orazio, C. Mancarella, E. Martuscelli, G. Sticotti, and G. Cecchin, "Isotactic polypropylene/ethylene-co-propylene blends: influence of the copolymer microstructure on rheology, morphology, and properties of injection-molded samples," *Journal of Applied Polymer Science*, vol. 72, no. 5, pp. 701–719, 1999.

[12] H. Tan, L. Li, Z. Chen, Y. Song, and Q. Zheng, "Phase morphology and impact toughness of impact polypropylene copolymer," *Polymer*, vol. 46, no. 10, pp. 3522–3527, 2005.

[13] T. Nedkov and F. Lednicky, "Morphologies of polyethylene-ethylene/propylene/diene monomer particles in polypropylene-rich polyolefin blends: flake structure," *Journal of Applied Polymer Science*, vol. 90, no. 11, pp. 3087–3092, 2003.

[14] A. van der Wal, A. J. J. Verheul, and R. J. Gaymans, "Polypropylene-rubber blends: 4. The effect of the rubber particle size on the fracture behaviour at low and high test speed," *Polymer*, vol. 40, no. 22, pp. 6057–6065, 1999.

[15] F. Laupretre, S. Bebelman, D. Daoust, J. Devaux, R. Legras, and J. L. Costa, "NMR, differential scanning calorimetry, and fourier transform infrared characterization of the crystalline degree and crystallite dimensions of ethylene runs in isotactic polypropylene/ethylene-propylene copolymer blends (iPP/EP)," *Journal of Applied Polymer Science*, vol. 74, no. 13, pp. 3165–3172, 1999.

[16] A. van der Wal, J. J. Mulder, J. Oderkerk, and R. J. Gaymans, "Polypropylene-rubber blends: 1. The effect of the matrix properties on the impact behaviour," *Polymer*, vol. 39, no. 26, pp. 6781–6787, 1998.

[17] H. G. Elias, *An Introduction to Plastics*, Wiley-VCH, Weinheim, Germany, 2nd edition, 2003.

[18] M. P. Luda, G. Ragosta, P. Musto et al., "Regenerative recycling of automotive polymer components: poly(propylene) based car bumpers," *Macromolecular Materials and Engineering*, vol. 288, no. 8, pp. 613–620, 2003.

[19] B. L. Fernandes and A. J. Domingues, "Caracterização mecânica de polipropileno reciclado para a indústria automotiva," *Polímeros: Ciência e Tecnologia*, vol. 17, no. 2, pp. 85–87, 2007.

[20] S. Hummel, *Atlas of Polymer and Plastic Analiysis*, vol. 2 part b/I, Carl Hanser, Weinheim, Germany, 1998.

[21] J. Karger-Kocsis and V. N. Kuleznev, "Dynamic mechanical and impact properties of polypropylene/EPDM blends," *Polymer*, vol. 23, no. 5, pp. 699–705, 1982.

[22] C. Grein, K. Bernreitner, and M. Gahleitner, "Potential and limits of dynamic mechanical analysis as a tool for fracture resistance evaluation of isotactic polypropylenes and their polyolefin blends," *Journal of Applied Polymer Science*, vol. 93, no. 4, pp. 1854–1867, 2004.

[23] M. Gahleitner, C. Grein, K. Bernreitner, B. Knogler, and E. Hebesberger, "The use of DMTA for predicting standard mechanical properties of developmental polyolefins," *Journal of Thermal Analysis and Calorimetry*, vol. 98, no. 3, pp. 623–628, 2009.

[24] M. Chen, C. Wan, W. Shou, Y. Zhang, Y. Zhang, and J. Zhang, "Effects of interfacial adhesion on properties of polypropylene/ wollastonite composites," *Journal of Applied Polymer Science*, vol. 107, no. 3, pp. 1718–1723, 2008.

[25] V. Delhaye, A. H. Clausen, F. Moussy, O. S. Hopperstad, and R. Othman, "Mechanical response and microstructure investigation of a mineral and rubber modified polypropylene," *Polymer Testing*, vol. 29, no. 7, pp. 793–802, 2010.

Journal of
Nanotechnology

BioMed Research
International

International Journal of
Corrosion

Smart Materials
Research

Journal of
Composites

International Journal of
Polymer Science

Journal of
Metallurgy

Journal of
Textiles

Hindawi

Submit your manuscripts at
http://www.hindawi.com

Journal of
Nanoparticles

Advances in
Materials Science and Engineering

Scientifica

Journal of
Nanomaterials

The Scientific
World Journal

International Journal of
Biomaterials

Journal of
Coatings

Journal of
Materials

Journal of
Crystallography

Journal of
Ceramics

Journal of
NANOSCIENCE